Open Journal of Modern Hydrology, 2026, 16(3), 299-325
https://www.scirp.org/journal/ojmh
ISSN Online: 2163-0496
ISSN Print: 2163-0461

Application of Analytical Hierarchy Process (AHP) and GIS Spatial Modelling for Flood Vulnerability Assessment in the Bonsa Catchment, Southwestern Ghana

Asare Asante-Annor*, Douglas Oti, Emmanuel Afful Oteng

Department of Geological Engineering, University of Mines and Technology (UMaT), Tarkwa, Ghana
Email: *aasante-annor@umat.edu.gh

How to cite this paper: Asante-Annor, A., Oti, D. and Oteng, E.A. (2026) Application of Analytical Hierarchy Process (AHP) and GIS Spatial Modelling for Flood Vulnerability Assessment in the Bonsa Catchment, Southwestern Ghana. *Open Journal of Modern Hydrology*, **16**, 299-325.
https://doi.org/10.4236/ojmh.2026.163017

Received: March 14, 2026
Accepted: July 24, 2026
Published: July 27, 2026

Abstract

Flash floods remain a major environmental hazard in Ghana, yet vulnerability assessments in rapidly developing municipalities receive limited attention compared to major urban centres such as Accra. This study applies an integrated Analytical Hierarchy Process (AHP) and GIS-based spatial modelling to delineate flood vulnerability zones within the Bonsa catchment in southwestern Ghana. Eight thematic layers of elevation, slope, drainage density, distance from drainage, landcover, geology, rainfall and population were standardised and weighted using AHP to reflect their relative influence on flood generation. The model achieved a Consistency Index (CI) of 0.121 and a Consistency Ratio (CR) of 0.086, confirming the reliability of expert judgements. Weighted overlay analysis produced five vulnerability classes: very high (0.9 km^2; 0.09%), high (113.2 km^2; 10.7%), moderate (587.8 km^2; 55.6%), low (352 km^2; 33.4%), and very low (1.94 km^2; 0.18%). Field-based historical flood points aligned strongly with the very high and high vulnerability zones, validating the model outputs. The most influential factors were rainfall intensity, slope, and elevation, while population distribution enhanced the spatial precision of vulnerability delineation. The drainage network exhibited a dendritic pattern with moderate drainage density, and land cover analysis revealed extensive built-up areas (57.4 km^2) and mined-out zones (48.1 km^2), both contributing to increased runoff. The study demonstrates that integrating AHP with GIS provides a cost-effective and robust framework for flood vulnerability assessment in developing municipalities. The resulting flood vulnerability map offers a valuable decision-support tool for watershed management, disaster preparedness, and sustainable spatial planning in the Bonsa catchment.

Keywords

Flood Vulnerability, Analytical Hierarchy Process (AHP), GIS Spatial Modelling, Watershed Management, Bonsa Catchment

1. Introduction

According to [1], floods are among the most devastating natural hazards. They impact human lives and cause severe economic damages throughout the world. And they occur when water levels overtop riverbanks, lakes, dams or dykes in low-lying areas during significant rainfall events. In recent times, the frequency and widespread damage caused by floods are on ascendency [2]. Floods by rainfall events are increasing as a result of climate change and their effects on societies are also getting worse [3]-[5]. The global disaster database, EM-DAT reveals that flood frequency and their causative storms are correlated with economic loss [2].

In view of this, flood risk mapping for residential areas is very critical, especially for newly developing communities. This elucidates the state of the ground for real estate and property developers as well as for the local residents to prepare or avoid their exposure to the inevitable. Flood risk assessment, a function of flood hazard, exposure, and vulnerability [6], is a tool that is often used by town planners, house insurers and banks for property and mortgage evaluations in many developed countries [7] and [8]. But this is something that is hardly considered in housing constructions as well as land property developments and evaluations in Ghana. And because of this, annual flooding with property damages; which are recurring are reported in many towns and cities in the country with several losses of lives [9] and [10]. With the shifting wind regimes and the increasing intensity of rainfall events observed in recent decades [11], flood frequency and magnitude are expected to rise across many catchments. It is therefore imperative that communities, planners, and policymakers remain fully aware of the evolving flood risks within their environments and the potential socio-economic and infrastructural consequences associated with such events. Awareness of flood risk and an understanding of its economic implications are essential for enabling individuals, communities, and decision-makers to take informed actions that can prevent disasters arising from avoidable exposure to inundation. This need is even more critical in low-income communities particularly rural villages and urban slums in Ghana where high poverty levels amplify vulnerability and limit the capacity to recover from flood-related losses.

Flood risk has been extensively assessed across different regions of the world using a wide range of methodological approaches. Mathematical and hydrological modelling techniques have been applied in countries such as Colombia, Crete (Greece), and Scotland [12]-[14]. Other studies have relied on surveys and community-based interviews to understand local perceptions of flood hazards, as demonstrated in Vietnam, Cyprus, Senegal, and Canada [15]-[18]. Machine-learning approaches have also been employed in India, Jordan, and Italy to enhance predictive accuracy [19]-[21]. Statistical analyses have been used in India, the United States, Laos, and Cambodia to quantify flood frequency and magnitude [22] and [23]. Additionally, modelling and simulation frameworks have been implemented in Belgium, England, and Pakistan [24] and [25], while GIS and remote sensing techniques have proven effective for spatial flood risk mapping, particularly in Pakistan [25]. Collectively, these methods have been applied either as standalone approaches or in combination, demonstrating the diversity and evolution of flood risk assessment techniques globally.

In Ghana, flood assessment and prediction remain limited despite the recurring and often devastating nature of flood events, which continue to result in significant loss of life and property [26] and [27]. Existing studies in the Western Region have largely focused on areas dominated by multinational mining companies, leaving residential communities where indigenous populations predominantly reside relatively understudied and poorly documented [28]. The absence of systematic flood studies and the scarcity of spatial data in these localities heighten the vulnerability of residents, exposing them to hazards such as intense rainstorms and subsequent flooding with severe socio-economic consequences.

This study therefore focuses on assessing flood vulnerability within the Bonsa River Basin, covering the Tarkwa-Nsuaem, Prestea-Huni Valley, Mpohor Wassa, and Twifo-Heman districts in the Western Region of Ghana. Communities within this basin experience recurrent annual flooding (personal communication), underscoring the need for a comprehensive spatial assessment. The study employs a GIS-based Analytical Hierarchy Process (AHP), a decision-support methodology that has been successfully applied in similar hydrological and environmental assessments [3] and [29], to identify and map high vulnerability flood zones within the Bonsa River Basin. The approach evaluates the relative influence of eight key flood-inducing factors namely, rainfall, slope, elevation, land cover, geology, distance from drainage, drainage density, population distribution, and historical flood occurrences by integrating expert-derived weights with spatial datasets. Model performance and spatial accuracy are further validated using field-based historical flood points, ensuring that the resulting vulnerability map reflects actual flood patterns observed within the basin. The resulting flood vulnerability map is intended to support informed decision-making for disaster preparedness, watershed management, land-use planning, and community resilience.

2. Description of Study Area

The Bonsa catchment, is a sub-catchment of the Ankobra River basin in Ghana, West Africa (**Figure 1**). It is located between longitudes 001˚41' and 002˚13' West and latitudes 005˚4' and 005˚43' North. The catchment straddles the intersection of four districts, namely: Twifo-Heman Lower Denkyira to the north, Tarkwa Nsuaem and the Prestea-Huni Valley to the west and Mpohor Wassa East to the east. The catchment has a generally low relief, with the elevations ranging between

30 m and 340 m above mean sea level and it drains an area of 1482 km^2.

The rainfall regime is bimodal, the major and minor rainfall seasons. The average peak of the major rainfall season falls between April and June; and the minor season between September and October. The rainfall ranges between 1578 mm and 1982 mm per annum with annual average minimum and maximum temperatures being 22˚C and 32˚C, respectively. Predominant land cover consists of evergreen and secondary forests, with scattered shrubs and farms. Between 1986 and 2011, deforestation rates have been increasing: 0.33% between 1986 and 1991, 0.70% between 1991 and 2002 and 2% between 2002 and 2011 [30].

The geology of the basin is characterised by Birimian and Tarkwaian rock systems [31], while the soil is composed mostly of ferric acrisols and forest oxysols according to the Ghana soil classification system [32]. Major economic activities in the catchment include open-pit gold mining, rubber cultivation and small-scale cocoa and food crop production.

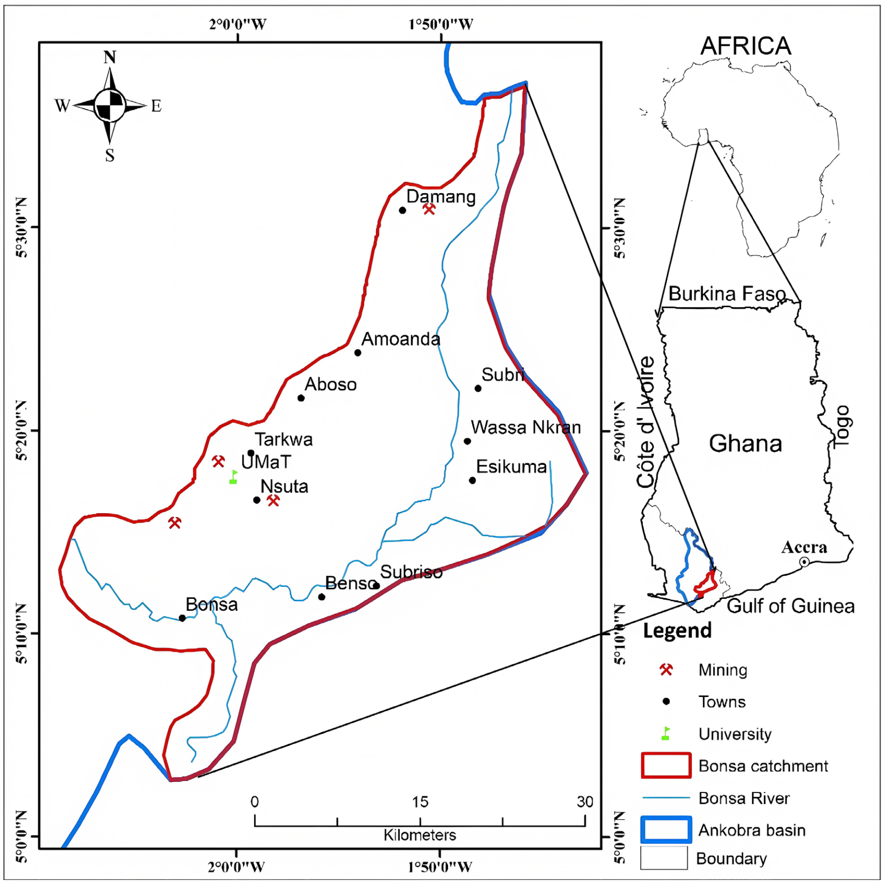

Figure 1. Location of Bonsa catchment, a sub-catchment of the Ankobra river basin in Ghana, west Africa.

3. Materials and Methods

3.1. Data Sources

Multiple datasets were assembled to support the flood vulnerability assessment of the Bonsa catchment. Topographic and hydrological parameters were derived from the ASTER Digital Elevation Model (DEM) provided by the United States Geological Survey (USGS) in March 2020. Land cover types were extracted from Landsat 8 OLI imagery and Google Earth geotiffs, which was acquired from USGS in March 2020. Geological units were obtained from the Ghana Geological Survey Agency (GGSA), as shapefiles in March 2020, while administrative boundaries and geographic distribution were sourced from the Survey Department of Ghana (SDG) in March 2020.

Rainfall data were collected from the Ghana Meteorological Agency (GMA) in CSV format in March 2020, covering the period 2005-2018 from stations at Tarkwa, Prestea, and Bogoso. Spatial rainfall surfaces were generated using Inverse Distance Weighting (IDW) interpolation in ArcGIS 10.8. Population data were obtained from the Ghana Statistical Service (GSS) in CSV format in March 2020, based on the 2021 Population and Housing Census, aggregated at the community level to produce population density maps.

Historical flood points were georeferenced during 2023 field surveys across 32 communities, using handheld GPS devices and validated against municipal disaster records and local accounts. These points were integrated into the vulnerability mapping to verify the accuracy of the AHP-derived zonation.

All datasets were standardised to UTM Zone 30 N (WGS 84) to ensure spatial consistency, and temporal harmonization was achieved by aligning rainfall (2005-2018), population (2021 census), and flood validation (2023 surveys) within a coherent analytical framework. Table 1 shows a detailed information on data sources used for this research.

Table 1. Data types and derived information.

Data Type	Format	Sources	Derived Data	Date
ASTER	DEM	USGS	Topographic and hydrological parameters	29/03/2020
Landsat 8 OLI and Google Earth	Geotiff	USGS	Land cover types	29/03/2020
Geological Map	Shapefile	GGSA	Geological units	20/03/2020
Topographic Map	Shapefile	SDG	Administration and geographic distribution	20/03/2020
Rainfall	csv	GMA	Rainfall distribution	20/03/2020
Population	csv	GSS	Population distribution	20/03/2020

Sources: USGS: United State Geological Survey; GGSA: Ghana Geological Survey Agency; SDG: Survey Department Ghana; GMA: Ghana Meteorological Agency; GSS: Ghana Statistical Service.

3.2. Methods

3.2.1. Multi-Criteria AHP

The various methods that have been used so far for flood vulnerability mapping in Ghana include questionnaires and interviews, hydrological model integrated into the GIS platform and supervised Random Forest (RF) classification [33] and [34]. This study however proposes a multi-parametric approach for delineating flood vulnerability in emerging and developed residential areas. The approach involves integration of Analytical Hierarchical Process (AHP) in a GIS mapping environment. The effectiveness of AHP applications in multiple, diverse criteria and measurement of trade-offs (sometimes using limited available data) in many interdisciplinary problems has led to its recognition across different fields [35].

In this study, flood vulnerability is considered to be a combination of physical and social vulnerability. In mathematical terms, flood vulnerability can be presented by Equation (1), whilst physical and social vulnerability are presented in Equation (2) and Equation (3) respectively.

$$\text{Flood vulnerability} = f\left(\text{physical vulnerability}, \text{social vulnerability}\right) \tag{1}$$

$$\begin{aligned}\text{Physical vulnerability} = f\big(&\text{geology}, \text{elevation}, \text{slope}, \text{rainfall}, \text{land cover}, \\ &\text{distance from drainage}, \text{drainage density}\big)\end{aligned} \tag{2}$$

$$\text{Social vulnerabilty} = f\left(\text{population}\right) \tag{3}$$

where f represents a function.

Now, following the order of steps in the AHP structure [3], the decision goal, as termed by [36], is flood vulnerability, with its subsequent criteria being physical vulnerability and social vulnerability. The elements of the criteria, as indicated in Equation (2) and Equation (3) are the first sub criteria in the brackets. The alternatives are very high, high, moderately high, low, and very low. They are also the ones that are weighted through comparison matrix to priority vector. And finally, by random index value method, a compliance rate is estimated.

The process of weighting the elements starts with assigning values based on relative importance of the elements by experts' opinions and information gathered from respondents in the study area. The values range from 1 to 9 (**Table 2**); whereby 1 means an equal contribution of the pairwise parameter and 9 means a very important parameter [36].

Table 2. Nine-point pairwise comparison scale [36].

Intensity of Importance	Definition	Explanation
1	Equal importance	Two elements contribute equally to the objective
3	Moderate importance	Experience and judgment slightly favor one parameter over another
5	Strong importance	Experience and judgment strongly favor one parameter over another
7	Very strong importance	One parameter is favored very strongly and is considered superior to another; its dominance is demonstrated in practice
9	Extreme importance	The evidence favoring one parameter as superior to another is of the highest possible order of affirmation
2, 4, 6, 8	Intermediate	When compromise is needed between two judgements

Note: Intermediate values can be used for parameters that are very close in importance.

The proposed method used $n \times n$ matrix and the comparisons of criteria, were from the expert judgment; literature review and historical flood zones land features. The weighting calculation follows Equation (4).

$$B = \begin{bmatrix} a_{1,1} & \cdots & a_{1,n} \\ \vdots & \ddots & \vdots \\ a_{n,1} & \cdots & a_{n,n} \end{bmatrix}, \tag{4}$$

where by $a_{kk} = 1, a_{lk} = \frac{1}{a_{kl}}, a_{kl} \neq 0$,

where B is the weight of the comparison criterion, a_{kl} (kl = (1,1), (1,2), ⋯, (n, n)). The right eigenvector (v) corresponding to the maximum eigenvalue ($\lambda_{\max}$) is calculated from the comparison criterion to normalize and find the relative weight (A_v) of the matrix by Equation (5).

$$A_v = \lambda_{\max} \cdot v \tag{5}$$

Also, the output of AHP has to be consistent for all the pairwise comparisons and is measured by Consistency Ratio (CR) and Consistency Index (CI). Where CI and CR are represented by Equation (6) and Equation (7).

$$CI = \frac{\lambda_{\max} - n}{n-1} \tag{6}$$

$$CR = \frac{CI}{RI}. \tag{7}$$

And where n is a number of criteria and RI is called Random Inconsistency index. The RI value for eight criteria (parameters) is 1.41 [29]. The maximum threshold of CI is ≤ 0.1 and CR ≤ 0.1 [36]. A rational value is attained when the CI and CR have fulfilled the maximum threshold value. The weight (local priority) for a criterion is calculated from a pairwise comparison matrix by dividing the value in each cell of each column by the sum of the values in the column, then averaging the new derived values in each row.

3.2.2. Vulnerability Index and Weights

Vulnerability measures the state of exposure of an object to a possibility of attack or damage. And to determine vulnerability indices, a weighted linear combination (WLC) is done by multiplying the weights assigned to elements of each criterion with the elements. And then aggregating the new weighted indicators or layers. Mathematically, vulnerability index can be defined as shown in Equation (8).

$$VI = \sum_{i=1}^{n} \sum_{j=1}^{n} W_i W_{ij} x. \tag{8}$$

where VI is vulnerability index, W_i and W_{ij} are weights of the ith and jth criteria and x is the element of the criteria.

3.2.3. Physical Vulnerability Analysis

Physical vulnerability as indicated in Equation (2) was segmented into elevation, slope, land cover, geology, rainfall, drainage density and distance from drainage. How the weights to the various elements in each criterion were assigned has been explained below.

Elevation

Topographic elevation is one of the most important criteria to consider when analysing flood tendencies of an area. Bonsa basin is mostly lowland with some few scattered highlands. As already known, lowlands are prone to flood during high rainfalls and so in this study, elevation of less than 50 m was assigned a high flood vulnerability zone weight while highlands with elevation greater than 200 m was assigned the least risk zone weight.

Slope

Land slope is also one of the criteria considered when analysing the flood vulnerability tendencies of the Bonsa basin. Naturally, flatlands are more likely to be flooded when there is excessive rainstorm than steeply sloping lands. For this reason, land slopes of less than 1.1^0 were given the highest flood vulnerability weight while those with gradients greater than 24^0 were given the least.

Land Cover

Land cover data set was categorised into rural settlement, still water, shrubs and farms, mining, and vegetation. The lands with settlements were given the highest vulnerability weight followed by the ones with ponds and still waters. The lands with vegetation cover were assigned the least vulnerability weight.

Distance from Drainage

The closeness of people and their properties to drainage channels is also a determinant to the risk of flooding. Areas located within 200 m of drainage channels were assigned the highest flood risk score (5), reflecting their direct exposure to inundation. The next class (200 - 350 m) was assigned a slightly lower score (4), indicating elevated but reduced risk compared to immediate streamside settlements. But those of 650 m and above were considered to be of least vulnerability and consequently, given the least weights.

Geology

The state of the geological features and the rock types in the basin are significant in assessing flood vulnerability tendencies of the basin. There are geological features that enable rainwater to penetrate through the rocks into the groundwater or prevents it from doing so, to become surface runoff. Those with features that enable runoff to occur are assigned higher weights than those that allow water penetrations. The Bonsa basin is geologically classified as the Tarkwaian and the Birimian rock systems. The Tarkwaian rock system being younger overlies the Birimian rock system. The Tarkwaian is sub-categorized stratigraphically as Huni sandstone, Tarkwa phyllite, Banket series, Kawere group, and intrusive rocks. The Birimian rock system is sub-categorized as metasediments and metavolcanics. These Birimian and Tarkwaian rock units controls infiltration capacity and subsurface drainage after a rainfall event through the differing permeability and their weathering behavior.

Rainfall

The Bonsa catchment experiences a humid tropical climate characterized by high rainfall intensity and marked seasonal variability. Annual rainfall typically ranges between 1500 and 2000 mm, with the wettest months occurring between April-June and September-October, corresponding to the major and minor rainy seasons in southwestern Ghana. Rainfall events are often short but intense, producing high runoff volumes that contribute significantly to flash flood occurrences in low-lying settlements. The spatial distribution of rainfall is influenced by local topography and prevailing wind systems, resulting in uneven precipitation patterns across the basin. These rainfall dynamics, coupled with land-use changes and soil characteristics, play a critical role in shaping flood vulnerability within the catchment.

Drainage Density

The Bonsa catchment exhibits a moderate drainage density, shaped by its dendritic network of streams and tributaries derived from the underlying Tarkwa Phyllite and Banket Series formations. This drainage pattern facilitates rapid runoff concentration during intense rainfall events, contributing to recurrent flash floods in low-lying settlements. The moderate density indicates a balance between infiltration and surface flow, yet the expansion of built-up areas and mined-out lands has altered natural hydrological responses, increasing runoff volumes and reducing the catchment's capacity to absorb stormwater. Consequently, drainage density plays a critical role in determining flood vulnerability across the basin.

3.2.4. Social Vulnerability Analysis

Population

The Bonsa catchment is characterized by a rapidly growing population, driven largely by mining activities, agricultural expansion, and urbanization in the Tarkwa Nsuaem, Prestea Huni Valley, Mpohor Wassa, and Twifo Heman districts. Settlements are concentrated in low lying areas and along river valleys, where land availability and economic opportunities attract residents despite the high flood vulnerability. The catchment hosts both indigenous communities and migrant populations, with dense residential clusters in mining towns such as Tarkwa and Prestea. This demographic pressure has intensified land use change, increased impervious surfaces, and heightened exposure to flood hazards, making population distribution a critical factor in delineating vulnerability zones.

3.2.5. GIS Spatial Modelling and Model Validation

The delineation of flood-prone areas was undertaken using the weighted overlay function in the ArcGIS Spatial Analyst environment, a technique widely and effectively applied in similar studies [37]. While hydrological hydraulic modelling remains the classical approach for flood vulnerability assessment, its application is often constrained in ungauged basins where data scarcity, high costs, and time requirements limit feasibility. In such contexts, GIS and remote sensing provide a practical alternative for delineating flood-prone zones.

In this study, remote sensing datasets including ASTER DEM and Landsat imagery were processed to derive key parameters such as elevation, slope, drainage density, distance from drainage, land cover, and geology (**Figure 2**). Rainfall and population data were incorporated to capture climatic variability and socio-demographic exposure. Each thematic layer was standardized and reclassified to ensure comparability across datasets. Weights were then assigned using the Analytical Hierarchy Process (AHP), reflecting expert knowledge of flood-causative factors. The weighted overlay analysis produced a preliminary flood vulnerability map that integrated physical, environmental, and social dimensions of flood vulnerability.

Model validation was conducted through ground surveys and comparison with historical flood occurrence points. This step enabled refinement of the classification scheme and confirmed the spatial accuracy of the outputs. The final flood vulnerability map thus represents a validated spatial product, providing a reliable basis for flood vulnerability assessment and management in the Bonsa catchment.

3.2.6. Analytical Hierarchy Process (AHP) Judgments

Pairwise comparisons for the Analytical Hierarchy Process (AHP) were obtained from nine experts with diverse technical and contextual backgrounds. The panel included two hydrogeologists, one GIS specialist, one environmental scientist, four staff members from the Geological Engineering Department of the University of Mines and Technology (UMaT), and one local water-resources officer. This composition ensured that the judgments reflected both scientific expertise and practical knowledge of flood vulnerability in the Bonsa catchment.

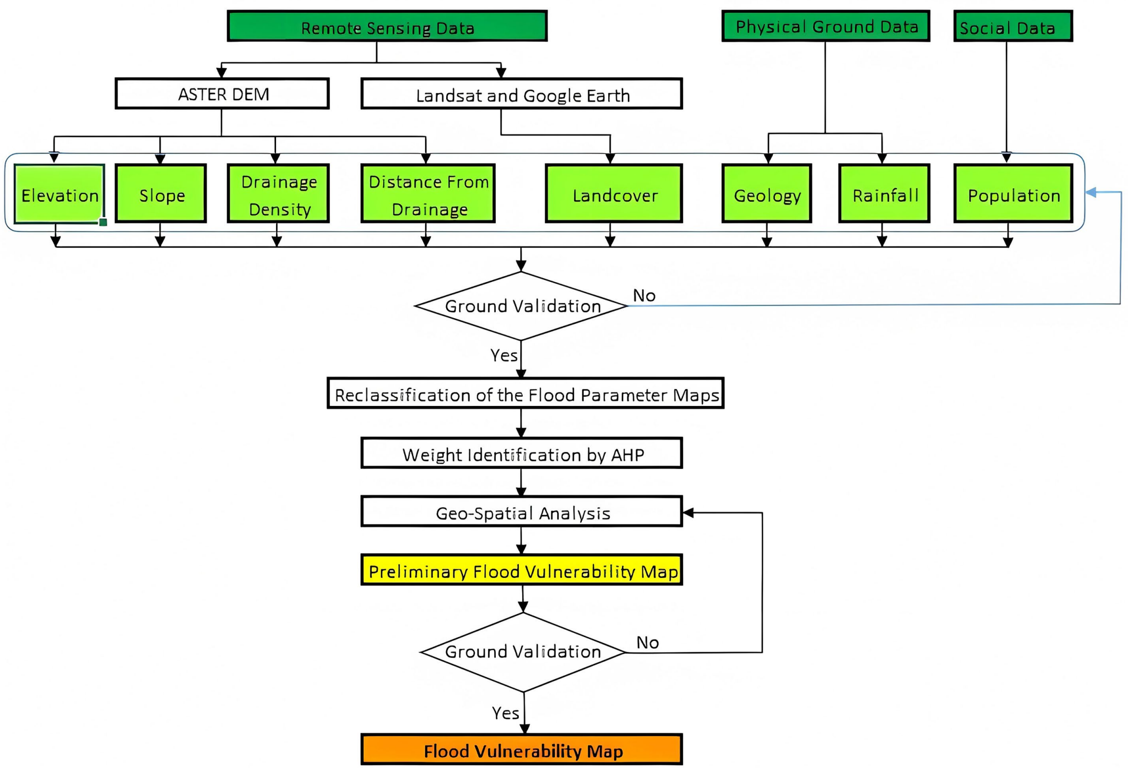

Figure 2. Flowchart process for flood vulnerability assessment.

Each expert was provided with a structured survey and participated in follow-up interviews to compare the relative importance of eight flood-inducing factors (rainfall, slope, elevation, land cover, geology, drainage density, distance from river, and population) using Saaty's 1 - 9 scale.

Consistency testing was performed by calculating the Consistency Index (CI) and Consistency Ratio (CR), both of which confirmed that the judgements were coherent and reliable for deriving factor weights.

4. Results

4.1. Ranking of Flood Vulnerability Factors by AHP

The Analytical Hierarchy Process (AHP) was applied to eight flood-inducing parameters namely slope, elevation, distance from drainage, drainage density, rainfall, geology, land cover, and population, resulting in 28 pairwise comparisons as shown in **Table 3** and Equation (9). The comparison matrix (**Table 4**), highlighted rainfall as the most influential factor, consistently rated higher against other parameters due to its direct role in runoff generation and flood occurrence. Slope and elevation followed closely, reflecting the importance of terrain gradient and altitude in controlling water flow and accumulation. Population and land cover ranked next, emphasizing the impact of settlement expansion, mining activities, and poor urban planning on flood exposure. Geology contributed moderately, influencing infiltration capacity and subsurface water movement, while distance from river and drainage density were ranked lowest, serving as secondary modifiers that refine spatial precision in flood vulnerability mapping. The derived weights and rankings confirm that rainfall, slope, and elevation are the dominant drivers of flood vulnerability in the Bonsa catchment, while socio-environmental and drainage factors provide complementary insights into localised risk.

$$\text{Number of comparisons} = \frac{n(n-1)}{2}, \quad n = 8 \tag{9}$$

$$N = 8$$

Table 3. Ranking of flood vulnerability parameters.

Parameter	S	E	DR	DD	R	G	LC	P
Slope (S)	1	2	5	6	1/2	5	5	3
Elevation(E)	1/2	1	3	5	1/3	5	3	3
D. River (DR)	1/5	1/3	1	3	1/5	1/3	1/3	1/3
D. Density (DD)	1/6	1/5	1/3	1	1/5	1/3	1/3	1/3
Rainfall (R)	2	3	5	5	1	5	4	2
Geology (G)	1/5	1/5	3	3	1/5	1	1/3	1/2
Landcover (LC)	1/5	1/3	3	3	1/4	3	1	1/2
Population (P)	1/3	1/3	3	3	1/2	2	2	1

Table 4. Weighted comparison table.

Parameter	S	E	DR	DD	R	G	LC	P	Priority	Percentage (%)
Slope (S)	0.22	0.27	0.21	0.21	0.16	0.23	0.31	0.28	0.236	24
Elevation(E)	0.11	0.14	0.13	0.17	0.10	0.23	0.19	0.28	0.169	17
D. River (DR)	0.04	0.05	0.04	0.10	0.06	0.02	0.02	0.03	0.046	5
D. Density (DD)	0.04	0.03	0.01	0.03	0.06	0.02	0.02	0.03	0.030	3
Rainfall (R)	0.43	0.41	0.21	0.17	0.31	0.23	0.25	0.19	0.276	27
Geology (G)	0.04	0.03	0.13	0.10	0.06	0.05	0.02	0.05	0.060	6
Landcover (LC)	0.04	0.05	0.13	0.10	0.08	0.14	0.06	0.05	0.081	8
Population (P)	0.07	0.05	0.13	0.10	0.16	0.09	0.13	0.09	0.102	10

From **Table 4**, the consistency index (*CI*) is determined using Equation (6),

$$CI = \frac{8.847 - n}{n - 1}, \quad n(N) = 8$$

$$CI = \frac{8.847099 - 8}{8 - 1}$$

$$CI = 0.121$$

Finally, the consistency ratio is computed using Equation (7),

$$CR = \frac{CI}{RI}$$

$$CR = \frac{0.121}{1.24}$$

$$CR = 0.09758$$

Both the consistency index (*CI*) and consistency ratio (*CR*) obtained are below the threshold values of 0.14 and 10% respectively. This indicates a high level of consistency in the pairwise judgments and implies that the determined weights are acceptable. **Table 5** shows a spreadsheet layout used to compute *CI* and *CR*.

Table 5. Consistency ratio results.

Sum	4.6	7.4	23.393	29	3.183	21.690	15.993	10.66
sum/Priority	1.086	1.247	1.065	0.878	0.879	1.303	1.297	1.092
$\lambda_{max} = \Sigma$(sum/Priority)				8.847				
$CI = (\lambda - n)/(n - 1)$	0.121							
RI	1.4							
$CR = CI/RI$	0.098							

4.2. Reclassification of Flood Vulnerability Parameters

A summary of the flood causative variables, their respective weights, and rankings is presented in **Table 6**. In the weight and ranking calculation step, the pairwise comparison matrix and the reclassified flood parameters were employed. Using a weighted linear combination, the assigned weights sum to 1, ensuring proportional representation of each factor in the overall vulnerability model. The Analytical Hierarchy Process (AHP) provided relative weights to the eight parameters, reflecting their influence on flood occurrence in the Bonsa catchment.

Rainfall emerged as the most dominant factor (weight = 27), underscoring its critical role in driving runoff and flash flood events. Slope (weight = 24) and elevation (weight = 17) followed, highlighting the importance of terrain gradient and altitude in determining flow accumulation and susceptibility. Population density (weight = 10) and land cover (weight = 8) refined the spatial distribution of risk, emphasizing the impact of settlement expansion, mining activities, and poor urban planning. Geology (weight = 6) influenced infiltration capacity, with formations such as Tarkwa Phyllite and Birimian Volcanics associated with higher vulnerability. Distance from drainage (weight = 5) and drainage density (weight = 3) provided additional spatial precision, identifying settlements within 200 m of streams and areas with moderate to high drainage density (>3.48 km/km^2) as particularly exposed.

Class breakpoints for rainfall, population, geology, slope, and distance from drainage were defined using basin specific hydrological reasoning and validated against regional literature. Higher scores were assigned to classes that increase flood susceptibility, such as high rainfall, dense population, impermeable lithologies, gentle slopes, and proximity to streams.

Rainfall (Weight = 27)

Rainfall classes were defined using observed station records (2005-2018) from Tarkwa, Prestea, and Bogoso. Breakpoints (>342 mm, 328 - 342 mm, 314 - 328 mm, 299 - 314 mm, <299 mm) reflect natural quartiles in seasonal rainfall distribution. Higher rainfall values were assigned higher scores (5) due to their direct role in runoff generation and flood occurrence. This approach is consistent with regional hydrological studies in Ghana [38] and [39].

Population (Weight = 10)

Population classes (<12,000 to >40,000) were derived from the 2021 Ghana Statistical Service census at community level. Higher population densities were scored higher (5) because densely populated settlements face greater exposure and vulnerability to flooding. This follows established disaster risk frameworks where population density is a proxy for exposure [40].

Geology (Weight = 6)

Geological classes were based on lithological units in the Bonsa catchment (Huni Sandstone, Tarkwa Phyllite, Banket Series, Kawere Group, Intrusive Rocks, Birimian Sediments, Birimian Volcanics). Units with low infiltration capacity (e.g., Tarkwa Phyllite, intrusive rocks) were scored higher (5), reflecting their tendency to promote surface runoff and flood susceptibility. More permeable formations (e.g., Banket Series) were scored lower (1). This classification aligns with basin-specific hydrogeochemical reasoning and previous work on infiltration capacity in Ghanaian aquifers [41] and [42].

Slope (Weight = 24)

Slope classes (<1.1˚, 1.1 - 5˚, 5 - 8.5˚, 8.5 - 24˚, >24˚) were derived from ASTER DEM data. Gentle slopes (<1.1˚) were scored highest (5) because they favour water accumulation and flood risk, while steep slopes (>24˚) were scored lowest (1) due to rapid runoff and reduced flood retention. This reasoning is consistent with terrain-driven flood susceptibility models [43] and [44].

Distance from Drainage (Weight = 5)

Distance classes (<200 m to >650 m) were defined using Euclidean distance from streams. Settlements within 200 m of drainage channels were scored highest (5), reflecting their direct exposure to flooding, while areas >650 m away were scored lowest (1). This approach follows basin-specific hydrological reasoning where proximity to streams is a key determinant of flood vulnerability [39].

Land Cover (Weight = 8)

Classes were based on Landsat 8 OLI imagery. Settlements were scored highest (5) due to impervious surfaces and poor drainage layouts. Mining areas were scored moderately (2) because disturbed land increases runoff but may have engineered drainage. Vegetation was scored lowest (1) as it enhances infiltration and reduces flood vulnerability.

Elevation (Weight = 17)

Classes (<50 m to >200 m) were derived from ASTER DEM. Low lying areas (<50 m) were scored highest (5) because they are prone to water accumulation and flooding. Higher elevations (>200 m) were scored lowest (1) as they are less susceptible to inundation. This classification reflects basin specific topographic controls on flood vulnerability.

The weighting structure demonstrates that rainfall, slope, and elevation are the primary flood inducing factors, while land use, geology, population, and drainage characteristics act as secondary modifiers that enhance the spatial delineation of flood vulnerability. These weights formed the basis of the weighted overlay analysis, producing a validated vulnerability map that integrates both physical and socio environmental drivers of flooding in the basin.

Table 6. Reclassification and weighting of flood parameters.

Parameters (units)	Class	Reclassification	Weight
Elevation (E)	<50	5	17
	50 - 100	4	
	100 - 150	3	
	150 - 200	2	
	>200	1	
Slope (D)	<1.1	5	24
	1.1 - 5	4	
	5 - 8.5	3	
	8.5 - 24	2	
	>24	1	

Continued

Drainage Density (km/km²)	>3.48	5	3
	1.38 - 2.02	4	
	0.86 - 1.38	3	
	0.34 - 0.86	2	
	<0.34	1	
Distance from Drainage (m)	<200	5	5
	200 - 350	4	
	350 - 500	3	
	500 - 650	2	
	>650	1	
Geology	Huni sandstone	4	6
	Tarkwa Phyllite	5	
	Banket Series	1	
	Kawere Group	2	
	Intrusive Rocks	5	
	Birimian sediments	3	
	Birimian Volcanics	3	
Land Cover	Settlement	5	8
	Still Water	4	
	Shrubs and Farms	3	
	Mining	2	
	Vegetation	1	
Rainfall	>342	5	27
	328 - 342	4	
	314 - 328	3	
	299 - 314	2	
	<299	1	
Population	>40,000	5	10
	30,000 - 40,000	4	
	20,000 - 30,000	3	
	12,000 - 20,000	2	
	<12,000	1	

4.3. Spatial Patterns of Flood Vulnerability Factors

Spatial patterns of flood vulnerability factors are shown in **Figures 3-10**. Analysis of the thirteen-year rainfall dataset (2005-2018) revealed marked seasonal variability, with areas experiencing higher rainfall intensities showing greater susceptibility to flooding compared to zones with lower precipitation. The slope map indicated that approximately 57 km² of the basin is level to near-level terrain, while 461 km² is characterized by gentle slopes. These flat terrains, when lacking adequate drainage, tend to accumulate floodwaters, increasing vulnerability. Elevation analysis showed that altitudes between 50 - 100 m dominate the catchment, covering about 496.2 km^2 (46.9%), whereas only 68.5 km^2 lies below 50 m, primarily in the southwestern sector. Population distribution maps highlighted the influence of mining activities in Tarkwa, where rapid population growth has placed pressure on sewage systems and driven poorer households to settle within floodplains, thereby heightening flood vulnerability.

Land cover analysis revealed dense urban settlements with poor planning layouts, further exacerbating flood vulnerability. Infiltration rates were found to be constrained by lithological characteristics, including rock type and overburden soils, with slow infiltration generating higher runoff and flash flood potential. The Euclidean distance map demonstrated that settlements located within or close to drainage channels are most prone to flooding, although effective drainage infrastructure can mitigate this risk. Finally, drainage density analysis showed that areas with moderate to very high density cover about 202 km^2 (18.9%) of the basin, where concentrated runoff pathways increase the likelihood of flood occurrence. Collectively, these spatial parameters underscore the complex interplay of rainfall, topography, land use, and population pressures in shaping flood vulnerability across the Bonsa catchment.

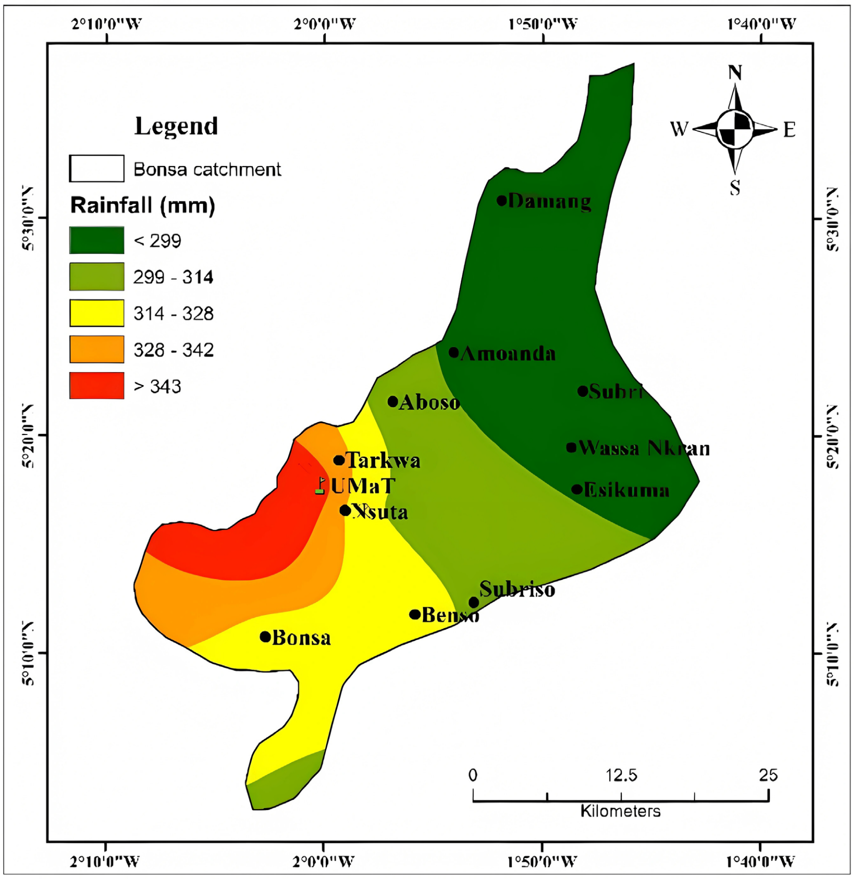

Figure 3. Spatial distribution of rainfall.

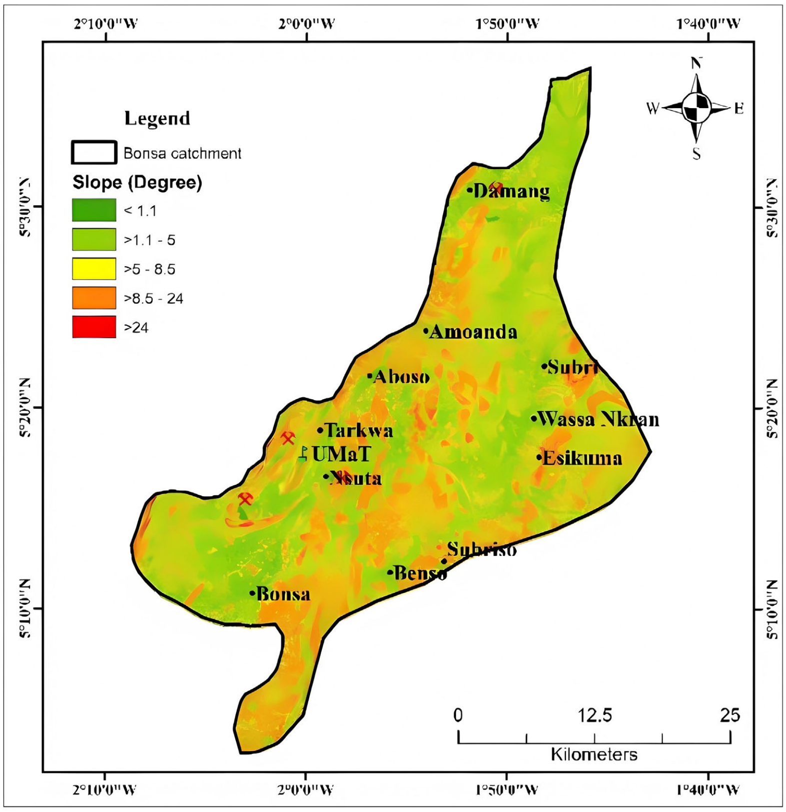

Figure 4. Spatial distribution of slope.

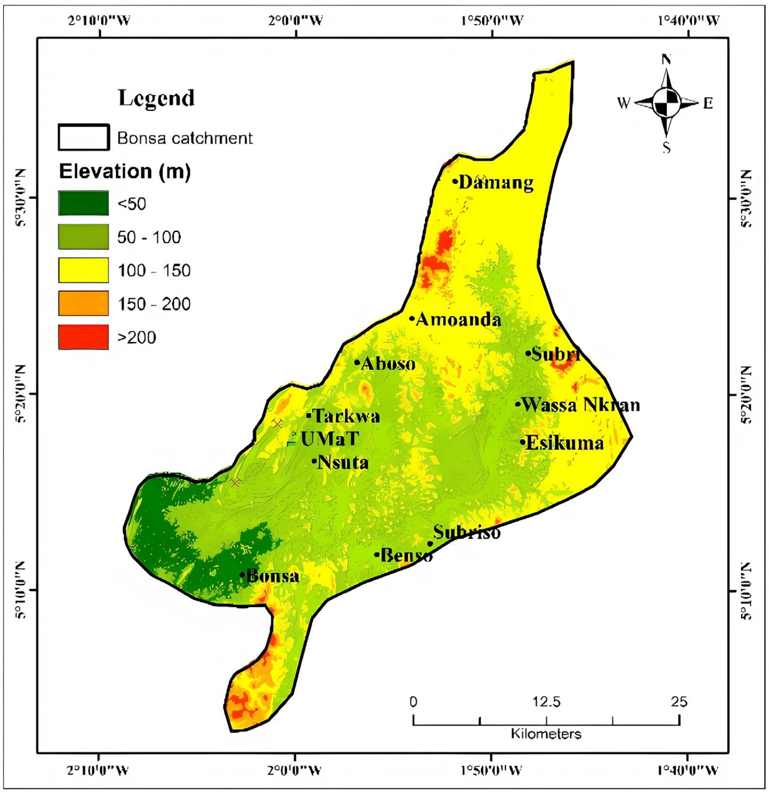

Figure 5. Spatial distribution of elevation.

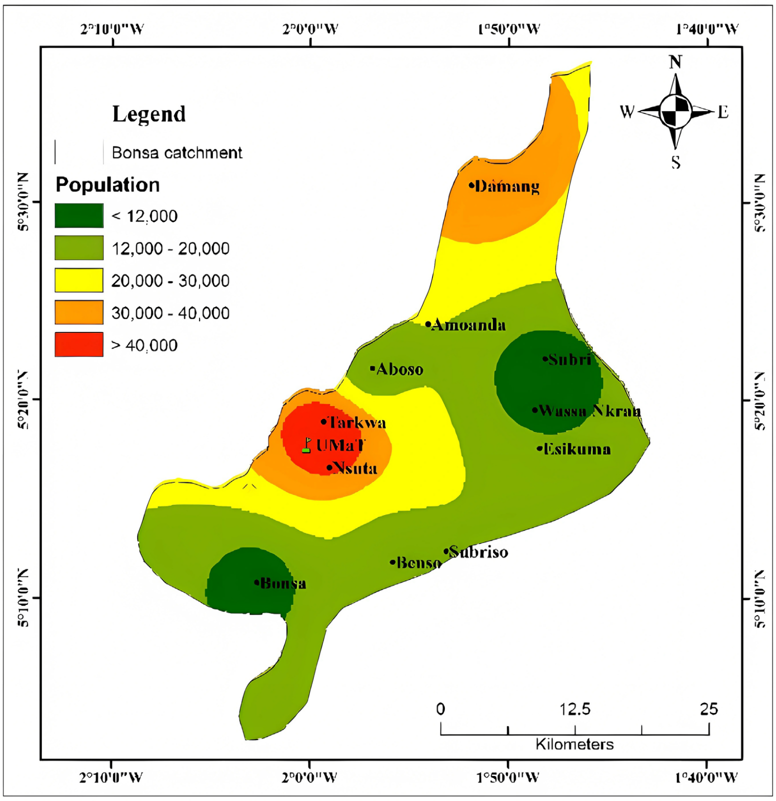

Figure 6. Spatial distribution of population.

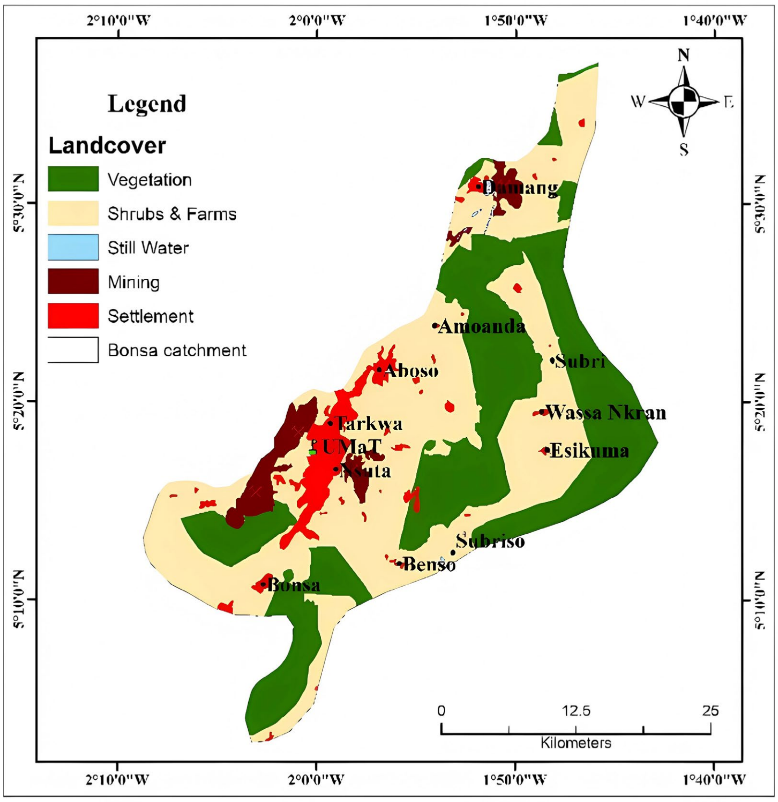

Figure 7. Spatial distribution of landcover.

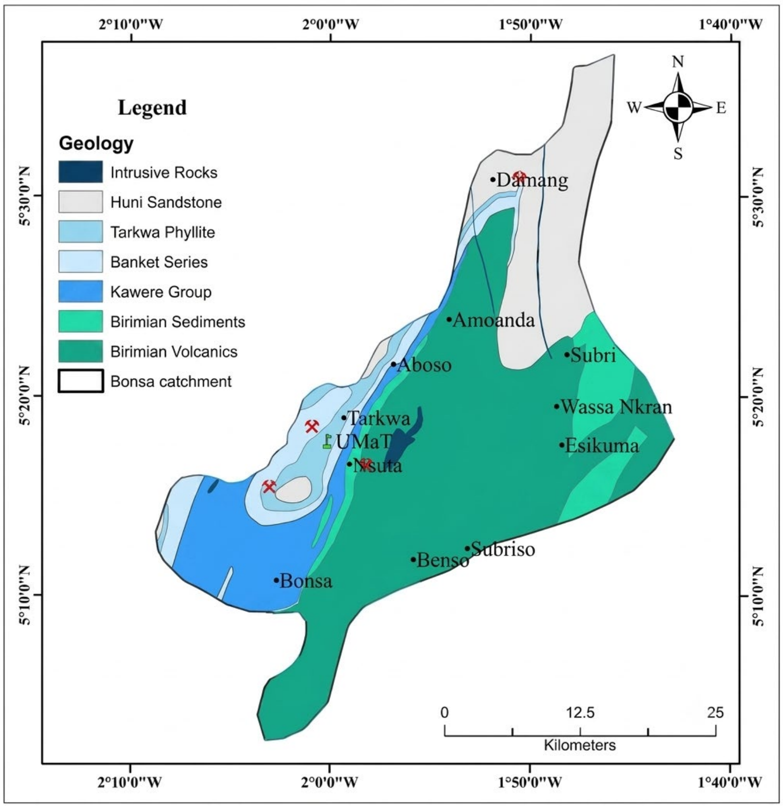

Figure 8. Spatial distribution of geology.

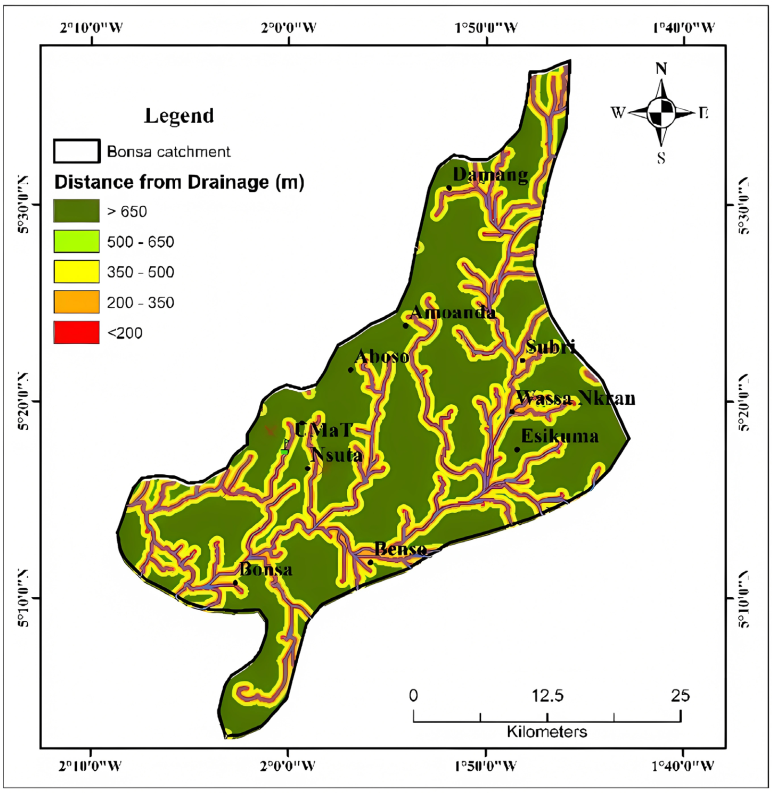

Figure 9. Spatial distribution of distance from drainage.

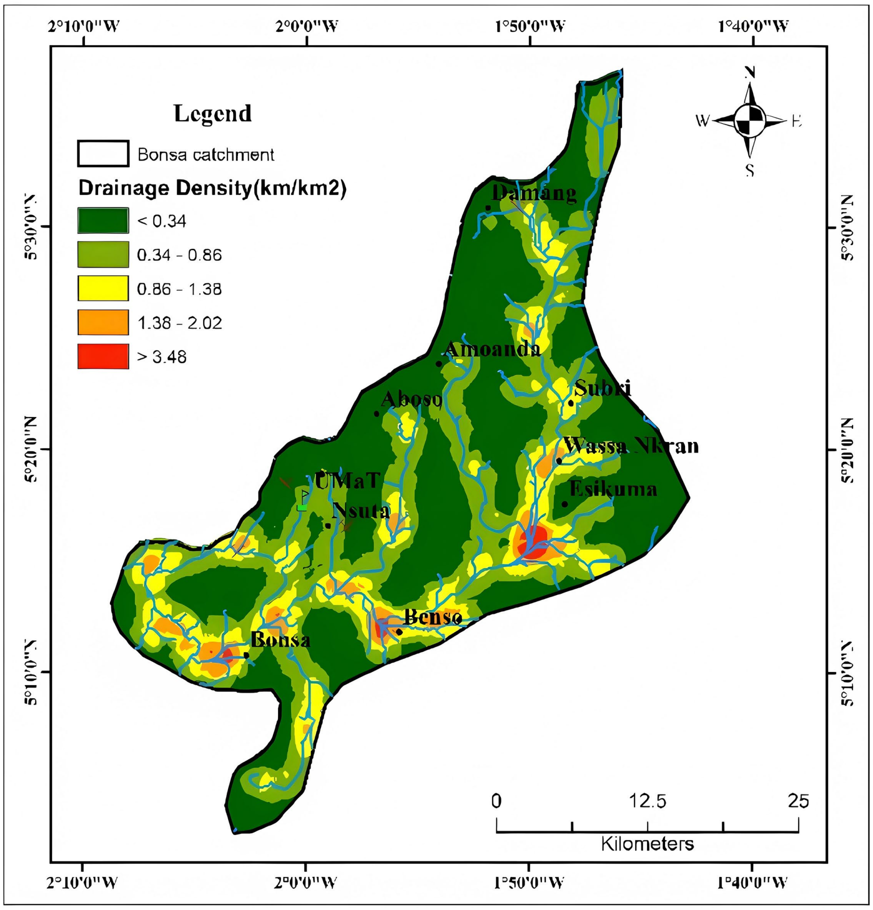

Figure 10. Spatial distribution of drainage density.

4.4. Flood Vulnerability Zonation for Bonsa Catchment

The final flood vulnerability map delineates five distinct zones of susceptibility within the Bonsa catchment (Figure 11 and Table 7). Areas classified as very high vulnerability cover approximately 0.895 km^2 (0.08%), representing densely settled low-lying terrain where severe flooding is recurrent. High vulnerability zones extend over 113.17 km^2 (10.71%), typically associated with settlements near drainage channels and regions of intense rainfall. The largest portion of the basin falls within the moderate vulnerability class, covering 587.76 km^2 (55.65%), where flood vulnerability is influenced by gentle slopes, moderate drainage density, and mixed land use. Low vulnerability areas account for 352.44 km^2 (33.37%), generally corresponding to higher elevations and vegetated landscapes with reduced runoff potential. Finally, very low vulnerability zones occupy only 1.94 km^2 (0.18%), reflecting terrain least affected by flood hazards.

This zonation highlights the spatial heterogeneity of flood vulnerability across the catchment, with rainfall, slope, and elevation exerting dominant control, while land cover, population distribution, and drainage characteristics refine localized vulnerability. The resulting map (Figure 11) provides a validated spatial framework for disaster preparedness, watershed management, and land-use planning in flood-prone communities of the Bonsa basin.

Table 7. Flood vulnerability classification and percentage area covered.

Vulnerability	Area	Percentage
Very high	0.895 km^2	0.08%
High	113.17 km^2	10.71%
Moderate	587.76 km^2	55.65%
Low	352.44 km^2	33.37%
Very Low	1.94 km^2	0.18%

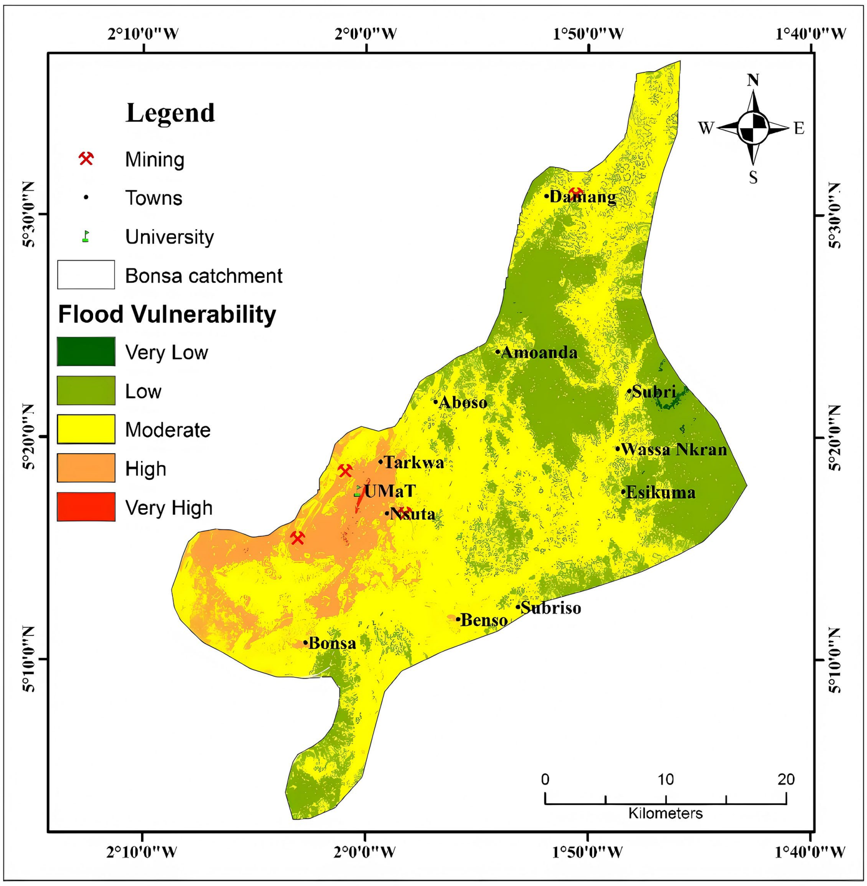

Figure 11. Flood vulnerability map of Bonsa catchment.

4.5. Flood Vulnerability Map Model Validation

Field surveys were conducted at 32 locations across the Bonsa catchment to validate the delineated flood prone zones. A team of experts engaged local residents and observed land features to verify the accuracy of the GIS based flood vulnerability map. The validation results (Table 8) show strong alignment between historical flood points and the model outputs, with most field observations corresponding to areas classified as high and very high vulnerability zones. Severe flooding was consistently reported in locations mapped as very high risk, while moderate and low zones exhibited only minimal or localised flooding (Figure 12). This close agreement between mapped vulnerability classes and ground observations confirms the reliability of the AHP GIS approach and demonstrates its effectiveness in integrating physical, environmental, and social parameters for flood vulnerability assessment in the Bonsa catchment.

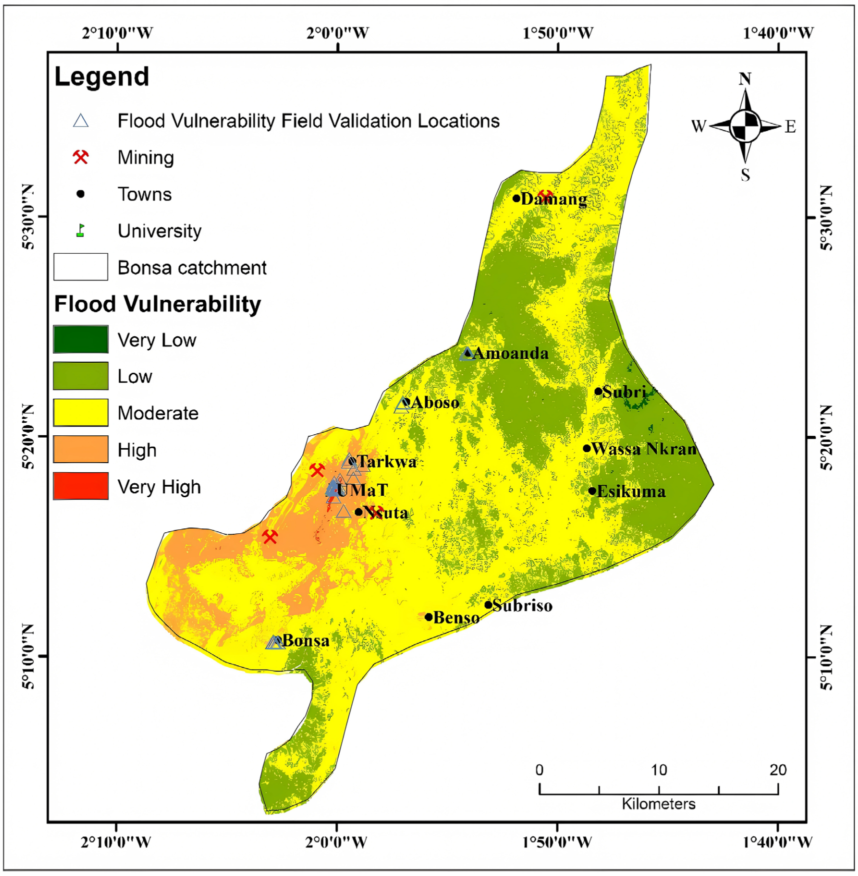

Figure 12. Flood vulnerability map of Bonsa catchment showing historical floods.

Table 8. Field results of historical floods within the Bonsa catchment.

Eastings	Nothings	On Map	On Ground	Field Observations
164042.5	67586.33	High	High	Flooding occurs
164847.3	70318.58	High	High	Some degree of flash flood
164910.1	71086.33	High	High	Flooding occurs
165649.6	71423.01	High	High	Flooding occurs
164511.3	71946.96	Very High	Very High	Severe flooding occurs
164449.2	71670.63	Very High	Very High	Severe flooding occurs
163245.7	69952.59	High	High	Severe flooding occurs
163584	69675.62	Very High	Very High	Severe flooding occurs
163738.7	70197.5	Very High	Very High	Severe flooding occurs
163344.2	69391.68	High	High	Some degree of flooding

Continued

163252	69514.69	High	High	Usually flood after heavy Down poor
163221.4	69637.6	High	High	Usually floods during rainfall
163128.9	69545.6	High	High	Usually floods during rainfall
158489.1	56560.74	High	Moderate	To a small extent of the river channel
158550.7	56560.64	High	Moderate	To a small extent of the river channel
158181.2	56622.67	High	Moderate	To a small extent of the river channel
158119.6	56592.06	High	Moderate	To a small extent of the river channel
158273.5	56530.38	High	Moderate	To a small extent of the river channel
168865.9	76324.45	Moderate	Low	Very minimal flooding at lower elevations
168989.5	76662.12	Moderate	Low	Very minimal flooding at lower elevations
168985.6	76631.11	Moderate	Moderate	Small levels of flash floods
169002.2	76687.33	Moderate	Moderate	Some degree of flooding occurs here
174483.3	80802.14	Moderate	Moderate	Flood occurs at the lower elevation
174357.7	80784.83	Moderate	Low	Very minimal flood
174452.9	80765.78	Moderate	Low	Very minimal flood
163559.7	69360.62	Very High	Very High	Flood always occurs
163559.7	69360.62	Very High	Very High	Flood always occurs
163559.7	69360.62	Very High	Very High	Flood always occurs
163559.7	69360.62	Very High	Very High	Flood always occurs
163436.5	69360.82	Very High	Very High	Flood always occurs
163405.7	69360.87	Very High	Very High	Flood always occurs
163189.3	68777.63	Very High	Very High	Flood always occurs

5. Conclusions

This study applied an integrated AHP-GIS multi-criteria approach to assess flood vulnerability within the Bonsa catchment, producing a spatially explicit and empirically validated flood vulnerability map for planning and disaster management. The weighted overlay analysis, based on eight thematic layers, revealed that rainfall, slope, and elevation exert the strongest influence on flood generation, while population distribution, geology, drainage density, and land cover significantly refine the spatial delineation of risk. The AHP model achieved a Consistency Index (CI) of 0.121 and a Consistency Ratio (CR) of 0.086, confirming the reliability of expert judgements.

The resulting vulnerability map classified the catchment into five zones: very high (0.9 km^2; 0.09%), high (113.2 km^2; 10.7%), moderate (587.8 km^2; 55.6%), low (352 km^2; 33.4%), and very low (1.94 km^2; 0.18%). Historical flood survey points corresponded strongly with the very high and high flood vulnerability zones, validating the model outputs. The high flood vulnerability areas are predominantly low-lying, densely settled zones underlain by clay-rich sediments of the Tarkwa Phyllite and Banket Series, which promote low infiltration and high runoff accumulation. Settlements located at the foot of surrounding hills experience recurrent flooding, while those on hilltops and hill faces remain largely unaffected.

The drainage network derived from ASTER DEM exhibits a dendritic pattern with moderate drainage density, indicating efficient runoff concentration during intense rainfall events. Land cover analysis further revealed extensive built-up areas (57.4 km^2) and mined-out/dump sites (48.1 km^2), both of which exacerbate surface runoff and reduce natural infiltration capacity. These findings highlight the critical role of land-use change in amplifying flood hazards in rapidly developing municipalities.

The study establishes that combining AHP with GIS provides a cost-effective, replicable, and robust framework for flood vulnerability assessment in data-scarce environments. The outputs offer valuable guidance for municipal planning, watershed management, infrastructure siting, early-warning systems, and disaster preparedness. Future research may integrate hydrodynamic modelling, climate-change projections, and higher-resolution datasets to enhance predictive accuracy and support long-term flood resilience strategies in the Bonsa catchment and similar developing regions.

Conflicts of Interest

The authors declare no conflicts of interest regarding the publication of this paper.

References

[1] Khan, S.I., Hong, Y., Wang, J., Yilmaz, K.K., Gourley, J.J., Adler, R.F., *et al.* (2011) Satellite Remote Sensing and Hydrologic Modeling for Flood Inundation Mapping in Lake Victoria Basin: Implications for Hydrologic Prediction in Ungauged Basins. *IEEE Transactions on Geoscience and Remote Sensing*, **49**, 85-95. https://doi.org/10.1109/tgrs.2010.2057513

[2] Formetta, G. and Feyen, L. (2019) Empirical Evidence of Declining Global Vulnerability to Climate-Related Hazards. *Global Environmental Change*, **57**, Article 101920. https://doi.org/10.1016/j.gloenvcha.2019.05.004

[3] Aydin, M.C. and Sevgi Birincioğlu, E. (2022) Flood Risk Analysis Using Gis-Based Analytical Hierarchy Process: A Case Study of Bitlis Province. *Applied Water Science*, **12**, Article No. 122. https://doi.org/10.1007/s13201-022-01655-x

[4] Atanga, R.A. and Tankpa, V. (2021) Climate Change, Flood Disaster Risk and Food Security Nexus in Northern Ghana. *Frontiers in Sustainable Food Systems*, **5**, Article 706721. https://doi.org/10.3389/fsufs.2021.706721

[5] Najibi, N. and Devineni, N. (2018) Recent Trends in the Frequency and Duration of Global Floods. *Earth System Dynamics*, **9**, 757-783. https://doi.org/10.5194/esd-9-757-2018

[6] Foudi, S., Osés-Eraso, N. and Tamayo, I. (2015) Integrated Spatial Flood Risk Assessment: The Case of Zaragoza. *Land Use Policy*, **42**, 278-292. https://doi.org/10.1016/j.landusepol.2014.08.002

[7] Nkwunonwo, U.C., Whitworth, M. and Baily, B.A. (2020) A Review of the Current Status of Flood Modelling for Urban Flood Risk Management in the Developing Countries. *Scientific African*, **7**, e00269. https://doi.org/10.1016/j.sciaf.2020.e00269

[8] Osti, R., Tanaka, S. and Tokioka, T. (2008) Flood Hazard Mapping in Developing Countries: Problems and Prospects. *Disaster Prevention and Management*: *An International Journal*, **17**, 104-113. https://doi.org/10.1108/09653560810855919

[9] Asante-Annor, A., Ansah, E. and Acherefi, K. (2020) Preliminary Flood Vulnerability and Risk Mapping of Koforidua and Its Environs Using Integrated Multi-Parametric AHP and GIS. 6*th UMaT Biennial International Mining and Mineral Conference*, Tarkwa, 5-6 August 2020, 91-102.

[10] Asumadu-Sarkodie, S., Owusu, P.A. and Jayaweera, M.P.C. (2015) Flood Risk Management in Ghana: A Case Study in Accra. *Advances in Applied Science Research*, **6**, 196-201.

[11] Bell, V.A. and Moore, R.J. (2000) The Sensitivity of Catchment Runoff Models to Rainfall Data at Different Spatial Scales. *Hydrology and Earth System Sciences*, **4**, 653-667. https://doi.org/10.5194/hess-4-653-2000

[12] Bocanegra, R.A. and Stamm, J. (2021) Evaluation of Alternatives to Optimize the Flood Management in the Department of Valle Del Cauca. *Journal of Applied Water Engineering and Research*, **9**, 1-19. https://doi.org/10.1080/23249676.2020.1787241

[13] Koutroulis, A.G., Tsanis, I.K. and Daliakopoulos, I.N. (2010) Seasonality of Floods and Their Hydrometeorologic Characteristics in the Island of Crete. *Journal of Hydrology*, **394**, 90-100. https://doi.org/10.1016/j.jhydrol.2010.04.025

[14] Vozinaki, A.E., Tapoglou, E. and Tsanis, I.K. (2018) Hydrometeorological Impact of Climate Change in Two Mediterranean Basins. *International Journal of River Basin Management*, **16**, 245-257. https://doi.org/10.1080/15715124.2018.1437742

[15] Nguyen, M.T., Sebesvari, Z., Souvignet, M., Bachofer, F., Braun, A., Garschagen, M., *et al*. (2021) Understanding and Assessing Flood Risk in Vietnam: Current Status, Persisting Gaps, and Future Directions. *Journal of Flood Risk Management*, **14**, e12689. https://doi.org/10.1111/jfr3.12689

[16] Charalambous, K., Bruggeman, A., Giannakis, E. and Zoumides, C. (2018) Improving Public Participation Processes for the Floods Directive and Flood Awareness: Evidence from Cyprus. *Water*, **10**, Article 958. https://doi.org/10.3390/w10070958

[17] Cissé, O. and Sèye, M. (2016) Flooding in the Suburbs of Dakar: Impacts on the Assets and Adaptation Strategies of Households or Communities. *Environment and Urbanization*, **28**, 183-204. https://doi.org/10.1177/0956247815613693

[18] Thistlethwaite, J., Henstra, D., Brown, C. and Scott, D. (2018) How Flood Experience and Risk Perception Influences Protective Actions and Behaviours among Canadian Homeowners. *Environmental Management*, **61**, 197-208. https://doi.org/10.1007/s00267-017-0969-2

[19] Paul, A. (2014) Flood Prediction Model Using Artificial Neural Network. *International Journal of Computer Applications Technology and Research*, **3**, 473-478. https://doi.org/10.7753/ijcatr0307.1016

[20] Al-Fawa'Reh, M., Hawamdeh, A., Alrawashdeh, R. and Jafar, M.T. (2021) Intelligent Methods for Flood Forecasting in Wadi Al Wala, Jordan. 2021 *International Congress of Advanced Technology and Engineering* (*ICOTEN*), Taiz, 4-5 July 2021, 1-9. https://doi.org/10.1109/icoten52080.2021.9493425

[21] Toth, E. and Brath, A. (2002) Flood Forecasting Using Artificial Neural Networks in Black-Box and Conceptual Rainfall-Runoff Modelling.

[22] Samantaray, S., Sahoo, A. and Agnihotri, A. (2021) Assessment of Flood Frequency Using Statistical and Hybrid Neural Network Method: Mahanadi River Basin, India. *Journal of the Geological Society of India*, **97**, 867-880.

https://doi.org/10.1007/s12594-021-1785-0

[23] Stedinger, J.R. and Griffis, V.W. (2008) Flood Frequency Analysis in the United States: Time to Update. *Journal of Hydrologic Engineering*, **13**, 199-204. https://doi.org/10.1061/(asce)1084-0699(2008)13:4(199)

[24] Craninx, M., Hilgersom, K., Dams, J., Vaes, G., Danckaert, T. and Bronders, J. (2021) Flood4castRTF: A Real-Time Urban Flood Forecasting Model. *Sustainability*, **13**, Article 5651. https://doi.org/10.3390/su13105651

[25] Ibrahim, M., Huo, A., Ullah, W., *et al.* (2025) An Integrated Approach to Flood Risk Assessment Using Multi-Criteria Decision Analysis and Geographic Information System. A Case Study from a Flood-Prone Region of Pakistan. *Frontiers in Environmental Science*, **12**, Article 1476761. https://doi.org/10.3389/fenvs.2024.1476761

[26] Ahadzie, D.K. and Proverbs, D.G. (2011) Emerging Issues in the Management of Floods in Ghana. *International Journal of Safety and Security Engineering*, **1**, 182-192. https://doi.org/10.2495/safe-v1-n2-182-192

[27] Tasantab, J.C., Gajendran, T., von Meding, J. and Maund, K. (2020) Perceptions and Deeply Held Beliefs about Responsibility for Flood Risk Adaptation in Accra Ghana. *International Journal of Disaster Resilience in the Built Environment*, **11**, 631-644. https://doi.org/10.1108/ijdrbe-11-2019-0076

[28] Osei, B.K., Ahenkorah, I., Ewusi, A. and Fiadonu, E.B. (2021) Assessment of Flood Prone Zones in the Tarkwa Mining Area of Ghana Using a GIS-Based Approach. *Environmental Challenges*, **3**, Article 100028. https://doi.org/10.1016/j.envc.2021.100028

[29] Dandapat, K. and Panda, G.K. (2018) A Geographic Information System-Based Approach of Flood Hazards Modelling, Paschim Medinipur District, West Bengal, India. *Jàmbá: Journal of Disaster Risk Studies*, **10**, a518. https://doi.org/10.4102/jamba.v10i1.518

[30] Aduah, M.S., Warburton, M.L. and Jewitt, G. (2015) Analysis of Land Cover Changes in the Bonsa Catchment, Ankobra Basin, Ghana. *Applied Ecology and Environmental Research*, **13**, 935-955. https://doi.org/10.15666/aeer/1304_935955

[31] Akabzaa, T.M., Jamieson, H.E., Jorgenson, N. and Nyame, K. (2009) The Combined Impact of Mine Drainage in the Ankobra River Basin, SW Ghana. *Mine Water and the Environment*, **28**, 50-64. https://doi.org/10.1007/s10230-008-0057-1

[32] Dwomo, O. and Dedzoe, C.D. (2010) Oxisol (Ferralsol) Development in Two Agro-Ecological Zones of Ghana: A Preliminary Evaluation of Some Profiles. *Journal of Science and Technology* (*Ghana*), **30**, 1-18. https://doi.org/10.4314/just.v30i2.60538

[33] Amoako, C. and Boamah, E.F. (2014) The Three-Dimensional Causes of Flooding in Accra, Ghana. *International Journal of Urban Sustainable Development*, **7**, 109-129. https://doi.org/10.1080/19463138.2014.984720

[34] Ghansah, B., Nyamekye, C., Owusu, S. and Agyapong, E. (2021) Mapping Flood Prone and Hazards Areas in Rural Landscape Using Landsat Images and Random Forest Classification: Case Study of Nasia Watershed in Ghana. *Cogent Engineering*, **8**, Article 1923384. https://doi.org/10.1080/23311916.2021.1923384

[35] Ouma, Y.O. and Tateishi, R. (2014) Urban Flood Vulnerability and Risk Mapping Using Integrated Multi-Parametric AHP and GIS: Methodological Overview and Case Study Assessment. *Water*, **6**, 1515-1545. https://doi.org/10.3390/w6061515

[36] Saaty, T.L. (2008) Decision Making with the Analytic Hierarchy Process. *International Journal of Services Sciences*, **1**, 83-98.

https://doi.org/10.1504/ijssci.2008.017590

[37] Rimba, A.B., Setiawati, M.D., Sambah, A.B. and Miura, F. (2017) Physical Flood Vulnerability Mapping Applying Geospatial Techniques in Okazaki City, Aichi Prefecture, Japan. *Urban Science*, **1**, 7. https://doi.org/10.3390/urbansci1010007

[38] Kortatsi, B.K. (2007) Hydrochemical Framework of Groundwater in the Ankobra Basin, Ghana. *Aquatic Geochemistry*, **13**, 41-74. https://doi.org/10.1007/s10498-006-9006-4

[39] Apambire, W.B., Boyle, D.R. and Michel, F.A. (1997) Geochemistry, Genesis, and Health Implications of Fluoriferous Groundwaters in the Upper Regions of Ghana. *Environmental Geology*, **33**, 13-24. https://doi.org/10.1007/s002540050221

[40] Edmunds, W.M., Shand, P., Hart, P. and Ward, R.S. (2002) The Natural (Baseline) Quality of Groundwater: A UK Pilot Study. *Science of the Total Environment*, **310**, 25-35. https://doi.org/10.1016/s0048-9697(02)00620-4

[41] Barcelona, M.J., Gibb, J.P., Helfrich, J.A. and Garske, E.E. (1985) Practical Guide for Groundwater Sampling. *Illinois State Water Survey Report of Investigation*, **74**, 1-94.

[42] Gale, I.N. and Robins, N.S. (1989) The Sampling and Monitoring of Groundwater Quality. *British Geological Survey Hydrogeology Report*, **89**, 1-35.

[43] Saaty, T.L. (1980) The Analytic Hierarchy Process: Planning, Priority Setting, Resource Allocation. McGraw-Hill.

[44] Forman, E. and Peniwati, K. (1998) Aggregating Individual Judgments and Priorities with the Analytic Hierarchy Process. *European Journal of Operational Research*, **108**, 165-169. https://doi.org/10.1016/s0377-2217(97)00244-0